

Surface Characterization Study of the Reduction of an Air-Exposed Pt₃Sn Alloy, IV

STEVEN D. GARDNER,* GAR B. HOFLUND,* AND DAVID R. SCHRYER†

*Department of Chemical Engineering, University of Florida, Gainesville, Florida 32611
and †NASA Langley Research Center, Hampton, Virginia 23665-5225

Received October 21, 1988; revised February 14, 1989

Ion scattering spectroscopy (ISS), angle-resolved Auger electron spectroscopy, and electron spectroscopy for chemical analysis (ESCA or XPS) have been used to examine the reduction (300°C under 1 Torr of H₂ for 1 h) of an air-exposed, polycrystalline Pt₃Sn alloy surface. Initially, the surface was covered with a thick tin oxide layer. The reduction resulted in a loss of oxygen particularly from the near-surface region, migration of Pt to the surface from a tin-depleted Pt region lying beneath the tin oxide layer, and reduction of tin oxide to metallic tin which alloys with the Pt which migrated to the near-surface region. ISS shows that the outermost atomic layer of the reduced surface contains a large amount of Pt which probably occupies vacancies left by oxygen. © 1989 Academic Press, Inc.

INTRODUCTION

Platinum/tin systems are important catalytic materials for hydrocarbon reforming (1–14) and low-temperature CO oxidation (15–17). The presence of tin alters the catalytic behavior of platinum so it is important to understand the nature of the platinum–tin interaction. A recent study by Hoflund *et al.* (18) has shown that a platinum–tin alloy forms when a platinized tin oxide film is reduced by annealing in vacuum. Davis and co-workers (19, 20) have reached similar conclusions in studies of alumina-supported platinum–tin hydrocarbon-reforming catalysts using electron spectroscopy for chemical analysis (ESCA or XPS) and *in situ* X-ray diffraction. Their X-ray diffraction patterns indicate that PtSn is the only alloy which forms regardless of relative Pt and Sn loading (21). Furthermore, alloy formation is completely reversible with oxidative and reductive treatments.

These recent studies (18–21) suggest the importance of characterizing Pt/Sn alloy surfaces since these surfaces may be responsible for the unique catalytic properties of Pt/Sn systems. Early studies by

Bouwman and co-workers (22–25) show that the surface compositions of PtSn and Pt₃Sn samples are readily altered by ion sputtering, annealing in vacuum, exposure to oxygen or exposure to hydrogen. More recent studies by Hoflund and co-workers (26–29) have focused primarily on the surface enrichment in tin of Pt₃Sn alloy surfaces caused by annealing in vacuum or oxygen exposure. These studies utilized angle-resolved Auger electron spectroscopy (ARAES) (30), high-energy-resolution Auger electron spectroscopy (HRAES) (31), scanning Auger microscopy (SAM), ion-scattering spectroscopy (ISS), and angle-resolved ESCA.

Relatively little work has been done on the reduction of oxidized Pt/Sn alloy surfaces. The purpose of the present study is to examine an air-exposed Pt₃Sn alloy surface before and after reducing the surface by annealing in hydrogen. ISS, ARAES, and ESCA results are presented.

EXPERIMENTAL

Details of the method used to prepare the Pt₃Sn sample were presented in an earlier part of this study (26). The sample was stored in argon until use. It was inserted

into the ultrahigh vacuum (UHV) system (base pressure of 10^{-11} Torr) and sputter cleaned until all C and O contamination was removed. Then the sample was exposed to air and reinserted into the vacuum system. After the oxidized sample was characterized, it was moved into a preparation chamber attached to the UHV system and reduced under 1 Torr of H_2 at $300^\circ C$ for 1 h. The heating was carried out using a special heating system (32) which did not expose any hot spots to the H_2 which would cause dissociation to atomic hydrogen. Thus, the effects of the reduction are due only to exposure to molecular hydrogen. The sample temperature was measured using an optical pyrometer. After reduction the sample was moved back into the UHV system without air exposure for further characterization.

ARAES, ISS, and ESCA were performed using a Perkin-Elmer PHI Model 25-270AR double-pass cylindrical mirror analyzer containing an internal electron gun and movable aperture as the charged parti-

cle energy analyzer. ARAES (30) was performed in the nonretarding mode using a 3-keV, $10\text{-}\mu A$ primary beam from an external, glancing incidence electron gun. The electron beam incidence angle was approximately 20° off the alloy surface plane. Rotation of the 90° -slotted aperture allowed for selection of emission angles of 75° to obtain more bulk-sensitive spectra and 20° to obtain more surface-sensitive spectra. ISS spectra were also collected in the nonretarding mode using a 147° scattering angle and pulse counting detection (33). Sputter damage was minimized through the use of a 1 keV, 100 nA $^4He^+$ primary beam defocused over an area of about 1 cm^2 . Both survey and high-resolution ESCA spectra were collected with Mg $K\alpha$ excitation in the retarding mode using 50 and 25 eV pass energies, respectively.

RESULTS AND DISCUSSION

An ISS spectrum taken after sample cleaning and air exposure is shown in Fig. 1a. This spectrum contains a predominant

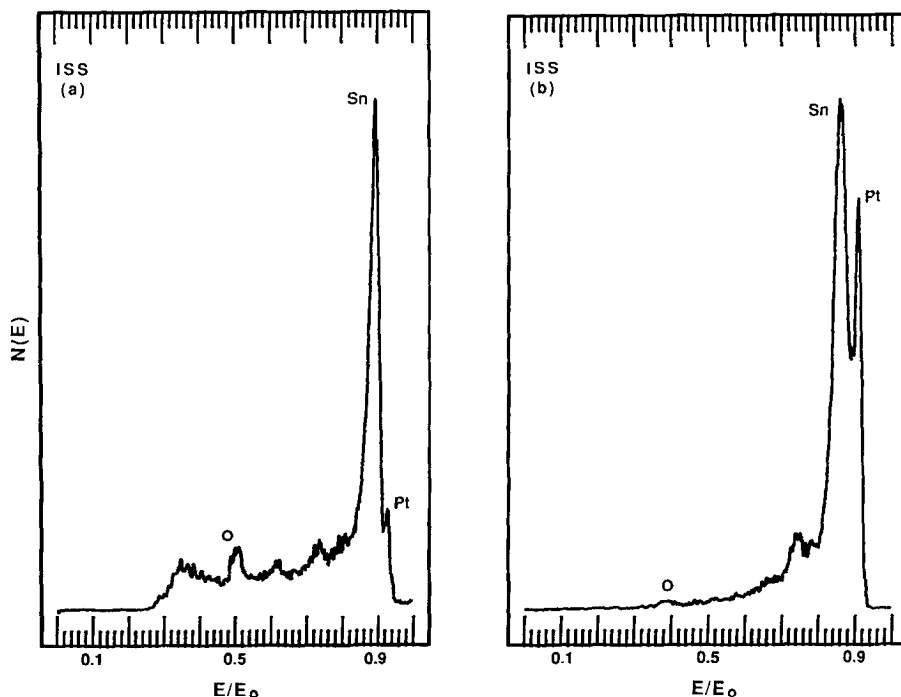


FIG. 1. ISS spectra taken from the polycrystalline Pt_3Sn sample after (a) sputter cleaning and exposing to air and (b) reducing the air-exposed sample under 1 Torr of H_2 for 1 h at $300^\circ C$.

peak due to Sn and very small peaks due to Pt and O. The O peak is shifted from its appropriate E/E_0 value of 0.4 to 0.5, the background is fairly large, and no ions are detected below an E/E_0 of 0.26. These facts indicate that the surface is oxidic in nature and that charging is occurring. This ISS spectrum is quite similar to that taken from an oxygen-exposed tin surface (34).

Annealing in hydrogen dramatically alters the composition of the outermost layer of atoms of the surface as seen in the ISS spectrum of Fig. 1b. The Pt peak has grown in size nearly to that of the Sn peak, the O peak is significantly decreased in size, the O peak appears at its predicted E/E_0 value of 0.4 indicating that charging is no longer a problem, and the inelastic background is reduced indicating that the outermost surface layer is more metallic in nature. Figures 1a and 1b were collected using the same instrument settings and are scaled accurately with respect to each other. Thus, the tin peak height does not change significantly during the reduction. The ISS cross section of O is much smaller than that of Pt (35). This suggests that the decrease in the number of O atoms may roughly correspond to the increase in the number of Pt atoms in the outermost surface layer. It is probable that the O atoms are removed from the surface layer through water formation during the reduction. Although speculative, it is possible that the Pt which migrates to the surface fills the vacancies left by the O. The chemical interaction between the Pt and H₂ provides a driving force for the Pt migration as discussed by Bouwman *et al.* (22) much like the chemical interaction between the Sn and O provides a driving force for Sn migration to the surface during an oxygen exposure (27–30). These studies also demonstrate that annealing a Pt/Sn alloy surface in vacuum rather than hydrogen enriches the near-surface region in Sn and not in Pt. A hydrogen environment is necessary to enrich the near-surface region in Pt.

Figure 2a shows a bulk-sensitive AES spectrum, and Fig. 3a shows a surface-

sensitive AES spectrum taken from the cleaned and air-exposed sample. Sn, C, and O peaks appear in these spectra, but no peaks due to Pt appear. This fact provides clear evidence that a fairly thick (>30 Å) layer of tin oxide forms over the Pt-rich region during the air exposure. The same conclusion has been reached in a previous study by Hoflund and Asbury (28) using angle-resolved ESCA. The O/Sn peak-height ratios in Figs. 2a and 3a are 0.61 and 0.58, respectively. These comparable values indicate that the composition of the tin oxide layer is fairly uniform with depth. The ratios are also typical of those obtained from tin oxide surfaces (36). The C peak is probably due to adsorption of hydrocarbons during the air exposure and always appears after exposing these samples to air.

Figures 2b and 3b show the bulk-sensitive and surface-sensitive AES spectra, respectively, taken after the reduction. Two changes due to the reduction are observed by comparing the bulk-sensitive AES spectra shown in Figs. 2a and 2b. The O/Sn ratio is substantially reduced and Pt migrates to the near-surface region during the reduction. Both of these facts are consistent with the ISS spectrum shown in Fig. 1b even though the bulk-sensitive AES probes more deeply beneath the surface than ISS. Comparing the surface-sensitive spectrum shown in Fig. 3b and the bulk-sensitive spectrum shown in Fig. 2b, it is seen that more Pt and less O are contained in the near-surface region than at greater depths. This observation supports the assertion that Pt replaces O which has been removed during the reduction. It is also possible to qualitatively describe the depth composition profiles of the Pt and O from these spectra. Initially, the O had a fairly uniform concentration through the oxidic region (of greater depth than that probed by the bulk-sensitive AES). After the reduction the O concentration is low at the surface and increases at greater depths. The Pt is more concentrated at the surface and less so at greater depths. It is seen that the increase in Pt and decrease in O in the

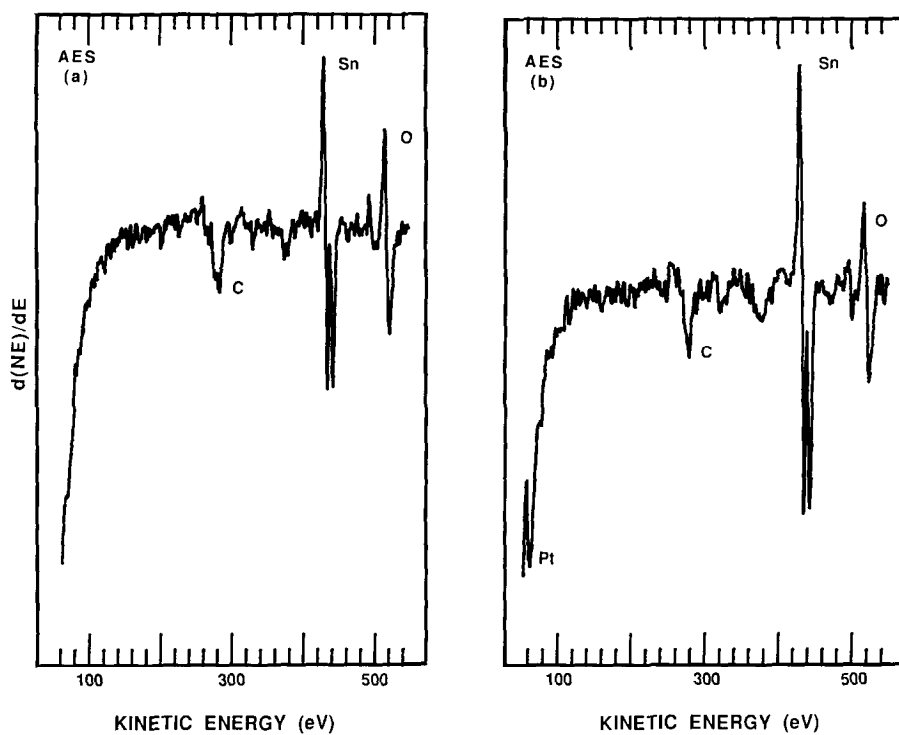


FIG. 2. Bulk-sensitive AES spectra taken from the (a) air-exposed and (b) reduced Pt_3Sn surfaces.

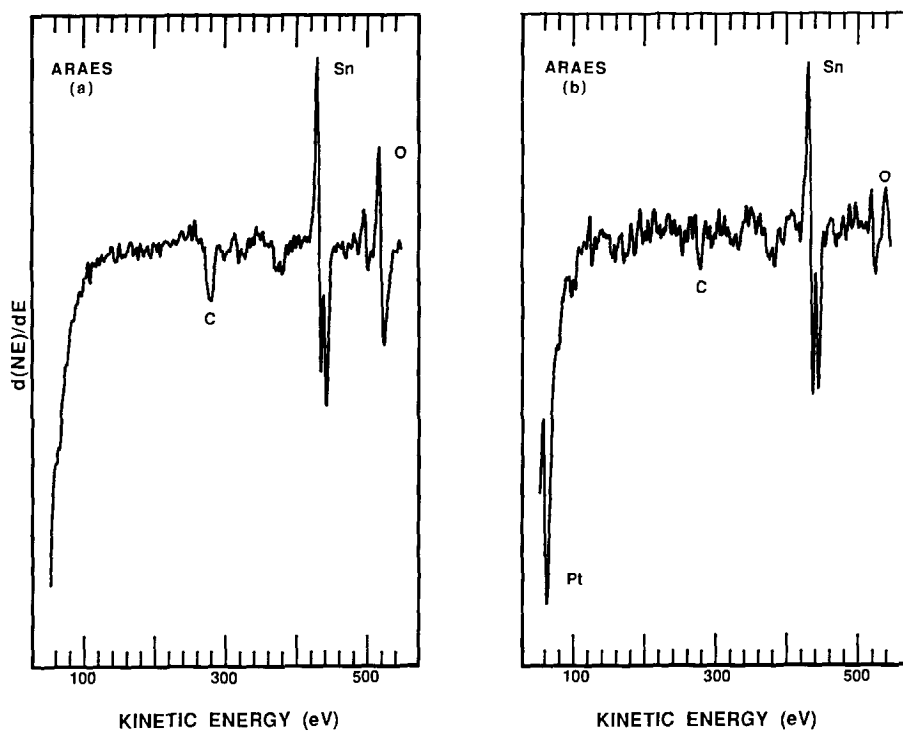


FIG. 3. Surface-sensitive ARAES spectra taken from the (a) air-exposed and (b) reduced Pt_3Sn surfaces.

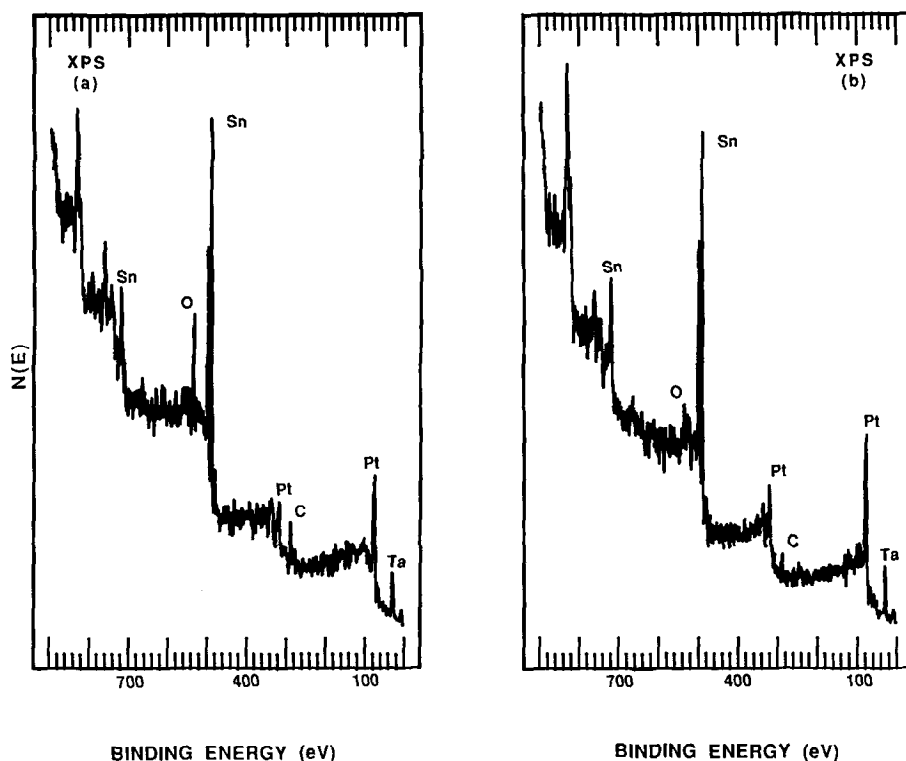


Fig. 4. ESCA survey spectra taken from the (a) air-exposed and (b) reduced Pt₃Sn surfaces.

near-surface region is large by comparing the surface-sensitive spectra shown in Figs. 3a and 3b.

ESCA survey spectra taken before and after the reduction are shown in Fig. 4a and 4b, respectively. Peaks due to Sn, O, Pt, C, and Ta are observed in the spectra. Ta appears because a Ta strip was used to hold the sample on the mounting block. ESCA probes more deeply than bulk-sensitive AES as observed by the presence of the large Pt 4f peaks in Fig. 4a. This Pt signal originates from a Sn-depleted region which lies beneath the tin oxide layer (28, 29). After the reduction the Pt peaks are increased and the O 1s peak is decreased. These results are consistent with both the ISS and AES spectra even though ESCA probes more deeply than the other two techniques.

High-resolution ESCA spectra of the Sn 3d, Pt 4f, and O 1s features before (A(a),

B(a), and C(a), respectively) and after reduction (A(b), B(b), and C(b), respectively) are shown in Fig. 5. The Sn 3d peaks shown in A(a) have a binding energy of 486.4 eV which corresponds to that of oxidic tin (SnO, SnO₂, or Sn hydroxides) (36, 37). However, these peaks are broad and contain a shoulder at about 485.0 eV which is due either to alloyed or to metallic tin lying beneath the oxide layer (28). After the reduction most of the Sn is in the form of alloyed or metallic Sn as evidenced by the peak position of about 485.3 eV. This value is larger than the Sn 3d binding energy of 484.6 eV for metallic Sn. Since a detailed deconvolution of these peaks has not been attempted in this study, a rigorous assignment of binding energies to species is not made. Further work on this topic is in progress. A higher binding energy shoulder at approximately 486.4 eV (shown as a dotted line) is also present after the reduc-

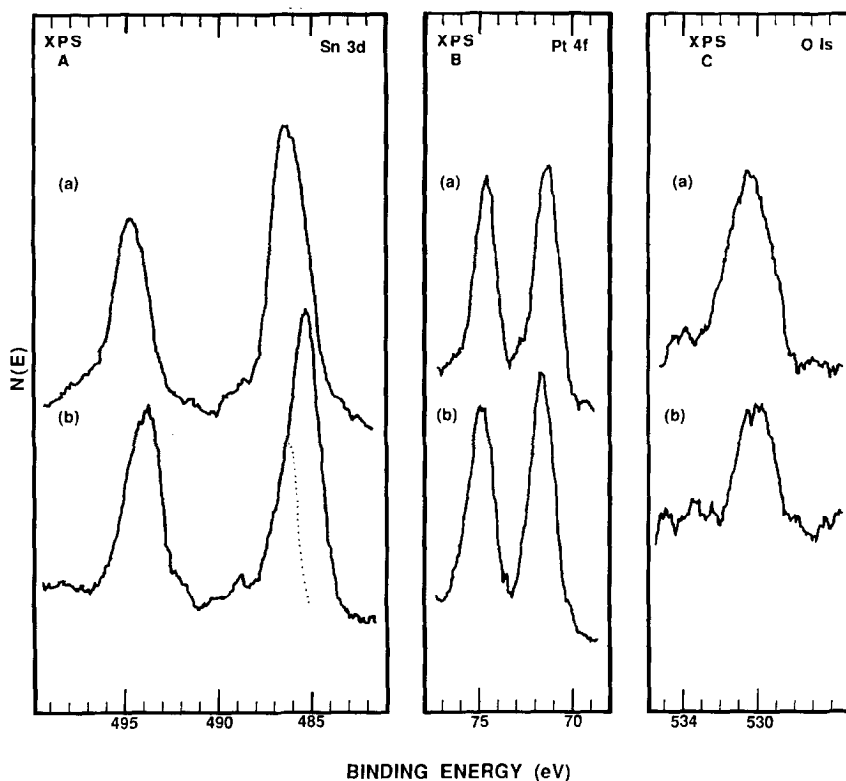


FIG. 5. High-resolution ESCA spectra taken from the (a) air-exposed and (b) reduced Pt_3Sn surfaces showing the (A) Sn 3d peaks, (B) Pt 4f peaks and (C) O 1s peak. The shoulder emphasized by the dotted line in A(b) is Sn in an oxidic form.

tion. This is consistent with the AES spectra shown in Figs. 2b and 3b, which show that most of the O lies beneath the surface.

The Pt 4f peaks shown in Fig. 5B(a) lie at a binding energy of 71.5 eV which is about 0.6 eV larger than that of metallic Pt. The width and shapes of these peaks suggest that only one chemical form of Pt contributes to this spectrum. As discussed above, this Pt is probably an Sn-depleted alloy, but the reason for the binding energy difference from metallic Pt is not currently understood. After reduction the Pt 4f binding energy is 71.7 eV. Again, it appears that only one chemical form of Pt is present. One possibility is that the Sn-depleted Pt alloy has a binding energy of 71.5 eV and that this binding energy increases to 71.7 eV as the Sn concentration increases after reduction of the alloy. Two studies (38, 39)

suggest that the Sn and Pt peaks obtained from an alloy are shifted to higher binding energy. This and other possibilities are being investigated.

Figure 5C(a) shows the ESCA O 1s peak taken from the air-exposed alloy surface, and Fig. 5C(b) shows the O 1s peak taken from the reduced alloy surface. The width and shape of the peak in Fig. 5C(a) indicates that two forms of O are present on the air-exposed sample: an oxidic form with a binding energy at 530.5 eV and hydroxyl groups with a binding energy at about 531.5 eV. The reduction process removes the hydroxyl groups leaving only the oxidic form beneath the surface.

CONCLUSION

ISS, ARAES, and ESCA have been used to examine an air-exposed, polycrystalline

Pt₃Sn surface before and after reduction by heating at 300°C under 1 Torr of H₂ for 1 h. Before reduction the surface was covered with a fairly thick (~40 Å), uniform layer of tin oxide and hydroxide. Beneath this layer was a Pt-rich region. ISS shows that the outermost atomic layer contains mostly Sn and O with only a very small amount of Pt present.

Reduction results in loss of O and enrichment in Pt of the near-surface region. ISS shows (1) that the outermost atomic layer is strongly enriched in Pt through migration of Pt to the surface, (2) that the outermost atomic layer becomes more metallic, and (3) that O is removed from the outermost atomic layer during the reduction. The ARAES data suggest that the Pt migrates to the surface from the Pt-rich region by moving through vacancies left by the oxygen which reacted with the hydrogen and desorbed, thus strongly enriching the outermost layer in Pt. ESCA shows that most of the tin oxide is reduced to metallic form and probably is present as alloyed Sn. The reduction results in loss of hydroxyl groups but a subsurface, oxidic form remains under the reductive conditions used. It is likely that reduction under the conditions used in this study but for longer periods would result in complete removal of the oxygen leaving a Pt-rich alloy at the surface.

ACKNOWLEDGMENT

Financial support for this research was received from NASA through Grant NAG-1-794.

REFERENCES

- Burch, R., *J. Catal.* **71**, 348 (1981).
- Burch, R., and Garla, L. C., *J. Catal.* **71**, 360 (1981).
- Burch, R., and Mitchell, A. J., *Appl. Catal.* **6**, 121 (1983).
- Muller, A. C., Engelhard, P. A., and Weisang, J. E., *J. Catal.* **56**, 65 (1979).
- Lieske, H., and Völter, J., *J. Catal.* **90**, 96 (1984).
- Bacaud, R., Bussiere, P., and Figueras, F., *J. Catal.* **69**, 399 (1981).
- Berndt, H., Mehner, H., Völter, J., and Meisel, W., *F. Anorg. Allg. Chem.* **49**, 47 (1977).
- Dautzenberg, F. M., Helle, J. N., Biloen, P., and Sachtler, W. M. H., *J. Catal.* **63**, 119 (1980).
- Völter, J., Lietz, G., Uhlemann, M., and Hermann, M., *J. Catal.* **68**, 42 (1981).
- Davis, B. H., *J. Catal.* **46**, 348 (1977).
- Li, Y.-X., and Klabunde, K. J., *Langmuir* **3**, 558 (1987).
- Palazov, A., Bonev, Ch., Shopov, D., Lietz, G., Sárkány, A., and Völter, J., *J. Catal.* **103**, 249 (1987).
- Coq, B., and Figueras, F., *J. Catal.* **85**, 197 (1984).
- Coq, B., and Figueras, F., *J. Mol. Catal.* **25**, 87 (1984).
- Stark, D. A., Cross, P. H., and Steward, G. J., *J. Phys. E. Sci. Instrum.* **16**, 158 (1983).
- "Closed-Cycle, Frequency-Stable CO₂ Laser Technology, Proceedings of Workshop at Langley Research Center, Hampton, VA, June 10-12, 1986" (C. E. Batten, I. M. Miller, and G. M. Wood, Jr., Eds.), NASA Conference Publication 2456.
- Schryer, D. R., Van Norman, J. D., Brown, K. G., and Schryer, J., submitted for publication.
- Gardner, S. D., Hoflund, G. B., Davidson, M. R., and Schryer, D. R., *J. Catal.* **115**, 132 (1988).
- Li, Y.-X., Stencel, J. M., and Davis, B. H. (1988) *React. Kinet. Catal. Lett.* **37**, 273 (1988).
- Stencel, J. M., Goodman, J., and Davis, B. H., in "Proceedings, 9th International Congress on Catalysis, Calgary, 1988" (M. J. Phillips and M. Ternan, Eds.), Vol. 3, p. 1291. Chem. Institute of Canada, Ottawa, 1988.
- Davis, B. H., personal communication.
- Bouwman, R., Toneman, L. H., and Holscher, A. A., *Surf. Sci.* **35**, 8 (1973).
- Bouwman, R., and Biloen, P., *Surf. Sci.* **41**, 348 (1974).
- Bouwman, R., and Biloen, P., *Anal. Chem.* **46**, 136 (1974).
- Biloen, P., Bouwman, R., Van Santen, R. A., and Brongersma, H. H., *Appl. Surf. Sci.* **2**, 532 (1979).
- Hoflund, G. B., Asbury, D. A., Kirszenstejn, P., and Laitinen, H. A., *Surf. Sci.* **161**, L583 (1985).
- Hoflund, G. B., Asbury, D. A., Kirszenstejn, P., and Laitinen, H. A., *Surf. Interface Anal.* **9**, 169 (1986).
- Hoflund, G. B., and Asbury, D. A., *Langmuir* **2**, 695 (1986).
- Asbury, D. A., and Hoflund, G. B., *Surf. Sci.* **199**, 552 (1988).
- Hoflund, G. B., Asbury, D. A., Corallo, C. F., and Corallo, G. R., *J. Vac. Sci. Technol. A* **6**, 70 (1988).
- Gilbert, R. E., Hoflund, G. B., Asbury, D. A., and Davidson, M. R., *J. Vac. Sci. Technol. A* **6**, 2280 (1988).
- Hoflund, G. B., and Corallo, G. R., submitted for publication.

33. Gilbert, R. E., Cox, D. F., and Hoflund, G. B., *Rev. Sci. Instrum.* **53**, 1281 (1982).
34. Asbury, D. A., and Hoflund, G. B., *J. Vac. Sci. Technol. A* **5**, 1132 (1987).
35. Parilis, E. A., in "Proceedings of the 7th International Conference on Phenomena in Ionized Gases, Belgrade, 1966" (B. Perović and D. Tosić, Eds.), Vol. 1 p. 129. Gradevinska Knjija Publishing House, Belgrade, 1966.
36. Hoflund, G. B., Grogan, A. L., Jr., Asbury, D. A., and Schryer, D. R., *Thin Solid Films* **169**, 69 (1989).
37. Hoflund, G. B., Asbury, D. A., and Gilbert, R. E., *Thin Solid Films* **129**, 139 (1985).
38. Paffett, M. T., and Windham, R. G., *Surf. Sci.* **208**, 34 (1989).
39. Cheung, T. T. P., *Surf. Sci.* **177**, L887 (1987).